Four New Variable Stars in the Field of KELT-16

Daniel J. Brossard
Department of Physics and Astronomy, Ball State University, 2000 West University Avenue, Muncie, IN 47306; DBrossard25@gmail.com

Ronald H. Kaitchuck
Department of Physics and Astronomy, Ball State University, 2000 West University Avenue, Muncie, IN 47306; rkaitchu@bsu.edu

Received October 27, 2020; revised December 8, 15, 2020; accepted December 17, 2020

Abstract We present three new variable stars in the field around the star KELT-16, and new period estimates for four previously known contact binary systems in this field, ASASSN-V J205658.12+314215.9, ASASSN-V J205552.88+314615.9, ZTF J205733.78+314612.6, and ZTF J205627.42+315322.4. Due to the short periods of these three new variable stars, and the shape of the light curves, we believe they are contact binary systems. In addition, we have found that the star Gaia DR2 1864883699097368448 is an additional variable star candidate and possibly an eclipsing binary eclipse candidate star.

1. Introduction

Binary systems are a common type of external variable star which can provide a great source of information about the stars in the pairing. Detached binary systems can provide mass and inclination estimates for the pair, while contact binary stars can provide a means to estimate the distance to the system (Rucinski 1994; Chen *et al.* 2018) along with being potential precursors to Type IIb Supernovae (Sravan *et al.* 2019).

Exoplanet transits are another type of external variable. Over 4,000 exoplanets have been found to date, with new discoveries being made every day. Based on recent transit occurrence rate studies that planets could potentially be common enough that there could be up to 0.18 habitable-zone planets per Sun-like star (Kunimoto and Matthews 2020), it's clear that there are many more planets left to be found.

Here we examine two previously known variable stars, ASASSN-V J205658.12+314215.9 and ASASSN-V J205552.88+314615.9, referred to as V1 and V2 respectively, discovered during the All-Sky Automated Survey for Supernovae (Shappee *et al.* 2014). Both stars are listed in the ASAS-SN Catalog of Variable Stars: VI (Jayasinghe *et al.* 2018, 2019).

In addition to these two ASAS-SN variables in this field, there are two other variable stars, ZTF J205733.78+314612.6 and ZTF J205627.42+315322.4, referred to as V5 and V6 respectively, that were announced in July as part of the Zwicky Transient Facility survey (ZTF) (Chen *et al.* 2020). We also discovered three new variable star candidates, labeled as V3, V4, and V7 in this paper. All three of these stars have Gaia and 2-MASS designations and but do not appear to have been the focus of any prior studies. Additional information on the new variable candidates is available in Table 4.

During our observations we detected one star that might have undergone a stellar or exoplanet transit of some kind. As with the variable star candidates it has Gaia and 2-MASS designations but again this star does not appear to have been the focus of any prior studies. Additional information is available in Table 6.

Table 1. Observation dates, filter used, and locations of our observations.

Observation Date (UT)	*Filter*	*Exposure Length (sec.)*	*Images Taken*	*Telescope*
2019-06-06	Cousins R	20	504	SARA-RM
2019-07-03	Cousins R	75	86	BSUO
2019-07-04	Cousins R	75	171	BSUO
2019-07-05	Cousins R	75	26	BSUO
2019-08-03	Cousins R	75	158	BSUO
2019-08-04	Cousins R	75	206	BSUO

2. Observations

Our observations of the region around the known planet hosting star KELT-16 (Oberst *et al.* 2017) were made using two different telescopes, the 0.5-meter at Ball State University Observatory (BSUO) in Muncie, Indiana, and the 1-meter at Observatorio del Roque de los Muchachos (SARA-RM) Observatory on La Palma in the Canary Islands. We obtained a total of 647 images using the FLI camera, cooled to between –28°C and –32°C and mounted on the BSUO telescope. A total of 504 images were taken with the Andor Ikon-L Camera, cooled to –49°C, mounted on the SARA-RM telescope. Between the two locations we had a total of 1,151 images (Table 1).

SARA-RM has a field of view of 11.62' (Keel *et al.* 2016), while the BSUO telescope has a field of view of 30.74'. Because of its large field of view several of the variable star candidates are only visible with the BSUO telescope. Additionally, only two potential comparison stars with known R-band photometry are visible in either of these fields. Unfortunately, the brighter of the two comparison stars was saturated in all of our images, leaving us with one usable comparison star.

Additionally, we used observations listed in the ASAS-SN database for stars V1 and V2. The survey had relatively few images of each field in the same night, leading to potential aliasing in the period estimates. Both stars have period estimates obtained using V-band images from the ASAS-SN survey, which has amassed at least 100 epochs for each field as of 2018. Additional information about these stars is available in Table 2. V1 had 173 magnitude measurements while V2 had 158 measurements listed in the ASAS-SN database as of the time of this paper. Because of the relatively few samples the periods of each should be examined further.

Table 2. Relevant information for the four known variable stars.[1]

Star	*R.A.* °	*Dec.* °	*Designation*	*ASAS-SN V-Mag.*	*ZTF. R-Mag.*	*Period (days)*	*Type*
ASASSN-VJ205658.12+314215.9	314.242	31.704	V1	14.62	—	0.7543	EW
ASASSN-VJ205552.88+314615.9	313.970	31.771	V2	14.29	—	0.6002	EW
ZTF J205733.78+314612.6	314.391	31.770	V5	—	16.35	0.4251	EW
ZTF J205627.42+315322.4	314.114	31.890	V6	—	16.93	0.2925	EW

[1] *Listed in the ASAS-SN catalog and the ZTF catalog. Additional information was from the Gaia mission via the NASA/IPAC Infrared Science Archive (IRSA, Jayasinghe* et al. *2018, 2019; Masci* et al. *2019; Chen* et al. *2020). It should be noted that neither the ASAS-SN nor the ZTF survey had errors assigned to their period estimates.*

Table 3. Information on the reference star.[1]

Comparison Star	*R.A.* *h m s*	*Dec.* ° ′ ″	*R mag*
TYC 2688-139-1	20 57 03.06	+31 42 43.3	12.03 ± 0.03

[1] *Listed in UCAC3 (Zacharias* et al. *2010).*

For V5 and V6 there were 69 G-band images and 68 Sloan R-band images listed in the ZTF Catalog of Periodic Variable Stars (Chen *et al.* 2020). Additional information about both of these stars is available in Table 2.

3. Analysis

3.1. Methodology

3.1.1. Initial image processing

The initial image processing was done using the CCDRED package of IRAF (Valdes 1988) to subtract the master bias, master dark, and the flat field correction. IRAF's SetJD tool was used to add the HJD date of the observations.

3.1.2. Variable detection

After the initial image processing was completed, we performed differential photometry with two different programs, AstroImageJ (AIJ) (Collins *et al.* 2017), and Variability Search Toolkit (VaST) (Sokolovsky and Lebedev 2017).

VaST is a program which specializes in finding objects undergoing brightness variations over the course of a set of observations. VaST operates by creating a source list and then does aperture photometry using the SExtractor program. VaST creates several variability indices for each source and compares it to other sources of similar brightness in order to flag potential variable candidates. VaST then generates a plot comparing the various variability indexes of each set of data. Candidate variable stars have a much higher variability index value than stars of similar instrumental magnitude. This plot feature also allows the user to examine the Individual light curves for any of the stars on the image. Additional information includes the location of the target in the image (Sokolovsky and Lebedev 2017).

AstroImageJ is a program that specializes in performing time-series differential photometry on specific targets. One of the main ways that AIJ differs from VaST is that the user selects the primary targets and the comparison stars to be used instead of every star in the field being compared to one another. This allows for shorter run times for creating the light curves (Collins *et al.* 2017). We had one usable R-band reference star Table 3), so AIJ provided a means to obtain standardized magnitude estimates for each of the stars of interest in the field.

3.1.3. Period determinations

Period estimates for each of the variable stars observed were found using the light curve and period analysis software Peranso 2.0 (Vanmunster 2006). Peranso contains several period analysis methods broadly broken into two categories: Fourier methods which attempt to fit the data to trigonometric functions, or statistical methods which compare individual points to one another. Our data were examined using a variety of methods to find the best-fit period for each variable star.

FALC (Fourier Analysis of Light Curves) (Harris *et al.* 1989) is a Fourier method used for both asteroid and variable star light curve analysis. It operates by breaking the light curve into segments and fitting them using Fourier analysis to fit a set of observations to a period (or phase) of the object's variations (Paunzen and Vanmunster 2016).

ANOVA (Schwarzenberg-Czerny 1996) Is a statistical method that uses orthogonal polynomials to analyze a set of observations. It uses multiple Fourier series to approximate the observation set (Paunzen and Vanmunster 2016; Vanmunster 2006).

PDM (Phase Dispersion Minimization) (Stellingwerf 1978) works by comparing the data to a series of trial frequencies which are then divided into bins. A variance is then calculated for each trial frequency and compared to the original data set (Paunzen and Vanmunster 2016; Vanmunster 2006).

3.2. Known variables in field

Prior to our observations four variable stars had been reported in the wider BSUO field. Two of the variable stars were found in 2018, with one of the two falling within the smaller SARA-RM field. Both are reported as being roughly 14th magnitude (V-band), and as contact binary systems (EW) (ASAS-SN; Jayasinghe *et al.* 2018). The other two previously known variable stars were 16th and 17th R-band magnitude, respectively, were found as part of the ZTF survey, and again are believed to be contact binary stars (Chen *et al.* 2020) (see Table 2).

The locations of the four previously discovered variable stars and the R-band reference star TYC 2688-139-1 are indicated in Figure 1.

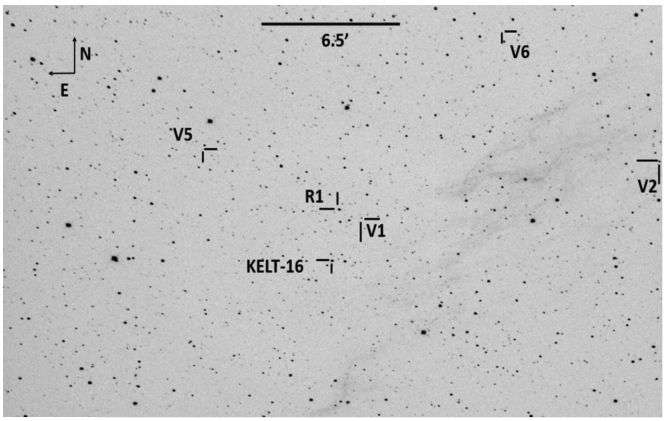

Figure 1. Finding chart for the four known variables in the field. They are labeled V1 (ASASSN-V J205658.12+314215.9), V2 (ASASSN-V J205552.88+314615.9), V5 (ZTF J205733.78+314612.6), and V6 (ZTF J205627.42+315322.4). The magnitude reference star TYC 2688-139-1 is marked as R1 on the image.

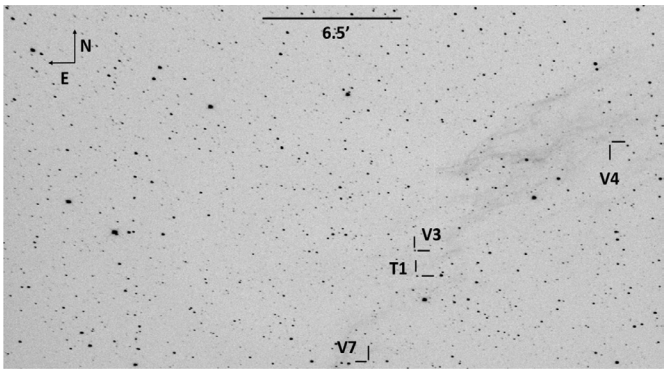

Figure 2. Finding chart for the four new variable star candidates. The image was taken on the night of 4 August 2019. 2MASS J20564622+3138394 is marked as V3, 2MASS J20560314+3145505 is marked as V4, and 2MASS J20565617+3131253 is marked as V7. The potential eclipsing binary candidate Gaia DR2 1864883699097368448 is marked as T1.

Table 4. Information for the three new variable star candidates.

Star	*Designation*	*R.A.*[1] °	*Dec.*[1] °
2MASS J20564622+3138394	V3	314.192	31.644
2MASS J20560314+3145505	V4	314.014	31.764
2MASS J20565617+3131253	V7	314.234	31.524

[1] *From Gaia Collaboration* et al. *(2016, 2018), NASA/IPAC (2020).*

3.3. Variable star candidates

Three new variable star candidates were found using VaST and then confirmed with AstroImageJ. The locations and other known information from the Gaia mission are presented in Table 4. The locations of the three candidate variable stars can be found in Figure 2.

3.4. Period estimates

3.4.1. V1 analysis

V1 refers to the known variable star ASASSN-V J205658.12+314215.9 in this paper. Analysis was done using our R-band images and V-band data taken from the ASAS-SN database.

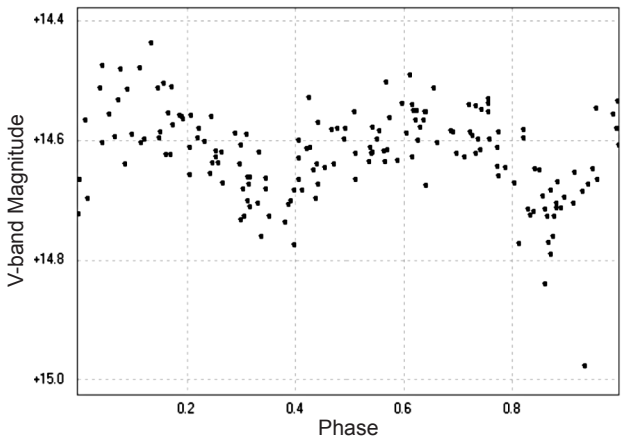

Figure 3a. V-band magnitude-phase plot for V1, showing the ASAS-SN data with the 0.7544 ± 0.0002-day period estimate from the FALC method.

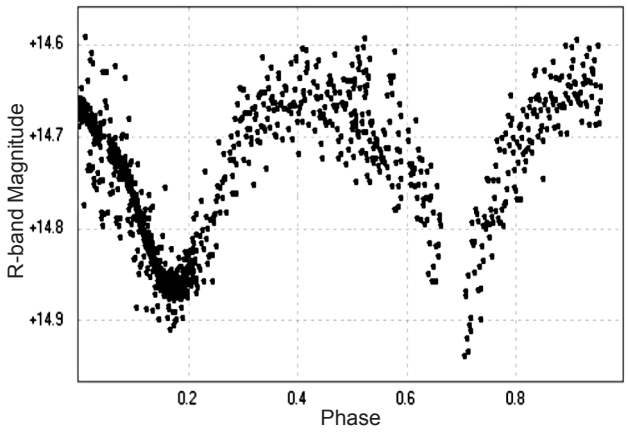

Figure 3b. R-band magnitude-phase plot for V1, showing the 0.7643 ± 0.0009-day period using the ANOVA method.

For the V-band analysis 173 images were used. The FALC method gave a period estimate of 0.7544 ± 0.0002 day (Figure 3a). This matches well the ASAS-SN period estimate of 0.7543 day.

For the R-band analysis a total of 1,110 images were used from the SARA-RM and the BSUO telescopes. From these measurements a mean apparent R-magnitude was determined to be 14.76 ± 0.02.

The Peranso R-band analysis of V1 yielded a period estimate of 0.7643±0.0009 day, found using the ANOVA method. This period can be seen in the magnitude-phase plot in Figure 3b. This is very close to the ASAS-SN period estimate and our estimate of 0.7544 day from the re-analysis of the V-band ASAS-SN data. Because the difference between the V-band and R-band analysis is larger than the error associated with our R-band measurements, there must be an additional reason for the difference. Based on the total number of images taken in each set, and the fact that the V-band data weren't taken using consecutive images but instead a single image per night over a long series of nights, we believe that correct period is closer to the R-band period.

It should be noted in Figure 3b that the more condensed grouping of data seen in the first minimum is due to those observations coming from SARA-RM, which had a much better signal-to-noise ratio than the observations obtained using BSUO.

3.4.2. V2 analysis

With V2, we were again able to do V-band and R-band analysis. Our V-band analysis using the ASAS-SN data found a best fit period of 0.8576 ± 0.0004 day using the PDM method.

Because of its smaller field of view the SARA-RM images of the KELT-16 did not include V2. The analysis was based on the 594 R-band images obtained with BSUO. From our measurements the mean R-magnitude was 14.08 ± 0.02.

Using the ANOVA method from Peranso gave a period estimate of 0.4388 ± 0.0005 day. This period estimate is fairly far from both the 0.600-day period from ASAS-SN and the 0.859-day estimate found in our reanalysis of the V-band photometry listed in the ASAS-SN database. We believe our R-band estimate is closer to the true period based on the larger data set used in the analysis. Additionally, unlike with our reanalyzed V-band ASAS-SN data, our R-band observations have a more noticeable difference in the sizes of the primary and secondary minima, as seen in Figure 4b.

3.4.3. V3 analysis

2MASS J20564622+3138394, now called V3, was near enough to KELT-16 that it was visible in the observations from both SARA-RM and the BSUO telescope, putting the number of R-band measurements available for its analysis at 1110. From these measurements we found that the mean apparent R-magnitude of V3 is 14.0 ± 0.02.

Using the ANOVA method, we arrive at a period estimate of 0.3465 ± 0.0005 day, as seen in Figure 5.

3.4.4. V4 analysis

The remaining four variable star candidates are located outside the field of the SARA-RM images. As such, 2MASS J20560314+3145505, now called V4, only appeared in the larger field of view offered by the BSUO telescope, leaving us with 594 R-band images. This star was much fainter than the previous three stars discussed, having a R-band magnitude estimate of 17.1 ± 0.02.

Because the star is so faint the analysis was done using a flux-phase plot instead of magnitude-phase. Because this star is much fainter the overall pattern showed up much better using flux-phase instead of with the magnitude-phase used for the three brighter stars. Figure 6 shows this data set for the best period found using the ANOVA method of 0.3022 ± 0.0006 day.

3.4.5. V5 analysis

As with V4, our only observations for ZTF J205733.78+314612.6, now called V5, were made at BSUO. The star's mean R-magnitude over the course of our observations was found to be 16.4 ± 0.02, which closely matches the magnitude listed for this star in the ZTF catalog of 16.347 (Chen *et al.* 2020).

We were able to confirm the variability of this star with our data and that it appears to be a contact binary as well. The analysis of our R-band images reveals a period estimate of 0.4282 ± 0.0007 day using the ANOVA method, which closely matches the ZTF survey period of 0.4251 day, as seen in Figure 7. Again, our result is close to the previously reported period estimate but they are outside of the error range. In this case we again believe our estimate is closer to the true period of this system because the number of observations used in our analysis was nearly ten times higher than those used in the ZTF survey's analysis, and because ours included more consecutive measurements as opposed to just a few images per night.

3.4.6. V6 analysis

We estimated that ZTF J205627.42+315322.4, now called V6, has a mean R-magnitude 16.9 ± 0.02. Again, our results closely matched those determined in (Chen *et al.* 2020), with their R-magnitude estimate listed at 16.926. Our analysis yields a period estimate of 0.2981 ± 0.0004 day using the PDM method as seen in Figure 8. This estimate closely matches up well with the period estimate obtained by the ZTF of 0.2925 day. As with the previous cases this estimate closely matches the period estimate made by the prior survey but is still outside of the error estimate. As with previous cases we again believe our estimate is closer to the true period of the system because of the larger amount of data used and because our data are made of consecutive images while it appears the ZTF data are not.

3.4.7. V7 analysis

We estimated 2MASS J20565617+3131253, now called V7, has a mean apparent R-magnitude of 17.7 ± 0.02, which makes it the faintest variable star candidate we've found in this search by over half a magnitude. Because it is so faint, we are only able to determine that V7 is likely a variable star, though we are less certain of its variability type. Figure 9 shows a sinusoidal pattern similar to the other candidate variable stars, though with a much lower signal to noise. It is possible that this is another contact binary star.

We used 582 R-band images to obtain our period estimate. The flux-magnitude plot can be seen in Figure 9. From the Peranso analysis we estimate this variable's period to be 0.2963 ± 0.0005 day using the ANOVA method.

3.4.8. Combined results

Table 5 contains the compiled period and magnitude estimates for each of the variable stars in the field. The R-band images for this analysis come from our own observations, while the V-band analysis was done using data listed in the ASAS-SN database.

3.5. Variable star candidate

In addition to the new variable star candidates listed in Table 5, there was one additional object of interest found. On the night of 6 June 2019 (UT) one other star in the field near Kelt-16 exhibited a variation in brightness. The location of this star, Gaia DR2 1864883699097368448, is marked in Figure 2. Following the same method as the other stars we calculated its R-band magnitude as 13.6 ± 0.02. Table 6 contains some of the previously known information about the star, mostly from the Gaia catalog.

Upon discovering this variation in our SARA-RM observations, we examined our five nights of observations from BSUO, but out of all of our observations the only ones to exhibit this change are our SARA-RM observations.

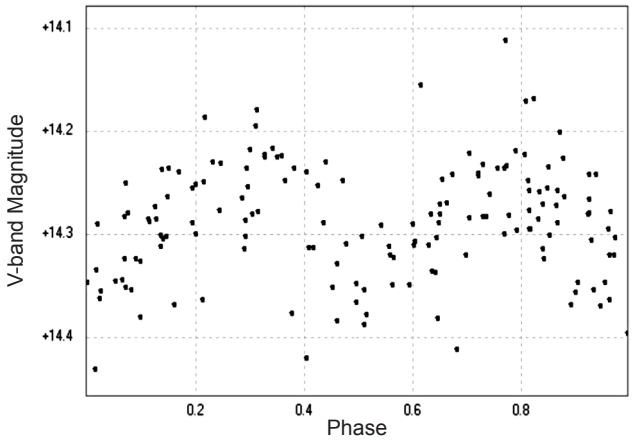

Figure 4a. V-band magnitude-phase plot for V2, showing the ASAS-SN data with the best fit period of 0.8576 ± 0.0004 day using the PDM method.

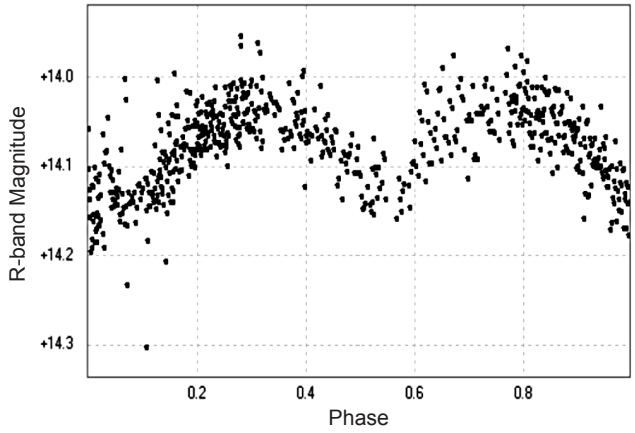

Figure 4b. R-band magnitude-phase plot for V2, showing the ANOVA method magnitude-phase plot of the period 0.4388 ± 0.0005 day.

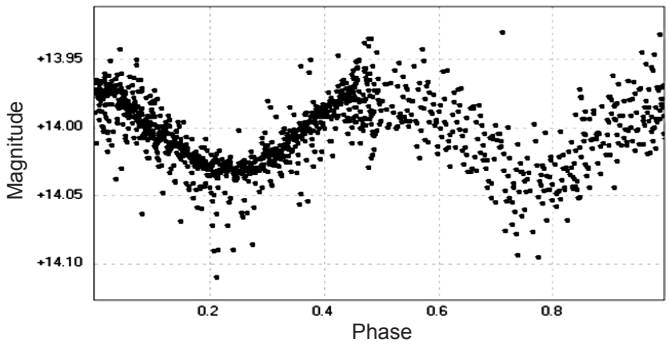

Figure 5. R-band magnitude-phase plot for V3, a period of 0.3465 ± 0.0005 day found using the ANOVA method. As noted in Figure 3b, the darker region in the first minimum is due to SARA-RM observations having a better SNR and so a smaller scatter in the data points.

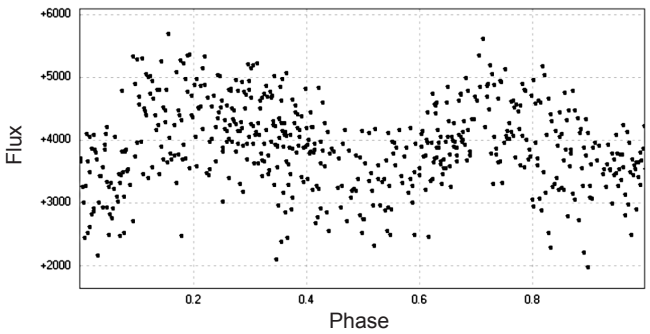

Figure 6. R-band flux-phase plot for V4 showing a period of 0.3022 ± 0.0006 day found using the ANOVA method.

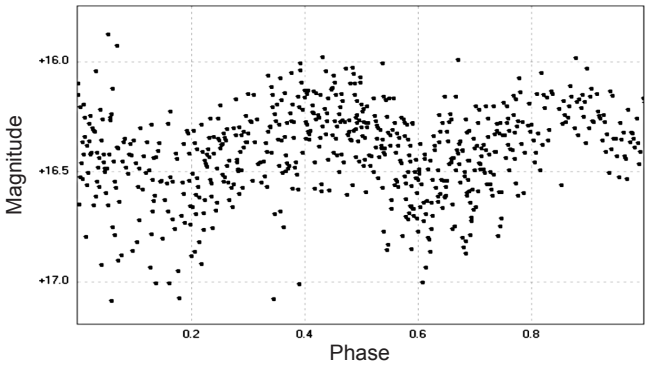

Figure 7. R-band magnitude-phase plot for V5. The flux-phase plot of our R-band data of V5 is for a period of 0.4282 ± 0.0007 day found using the ANOVA method.

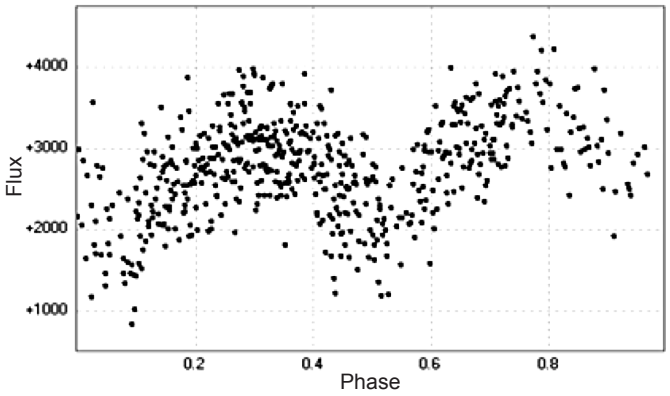

Figure 8: R-band flux-phase plot for V6, showing a period of 0.2981 ± 0.0004 day found using the ANOVA method.

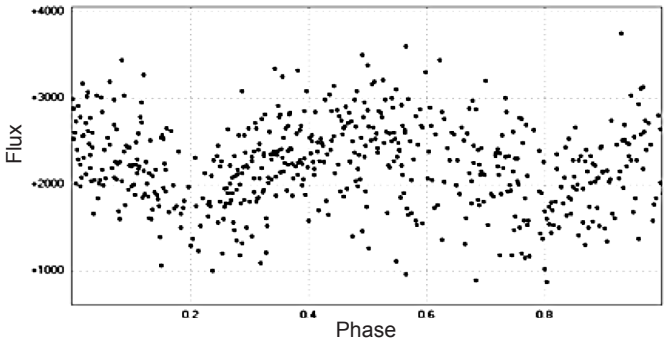

Figure 9. R-band folded flux-phase plot for V7, showing a period of 0.2963 ± 0.0005 day found using the ANOVA method.

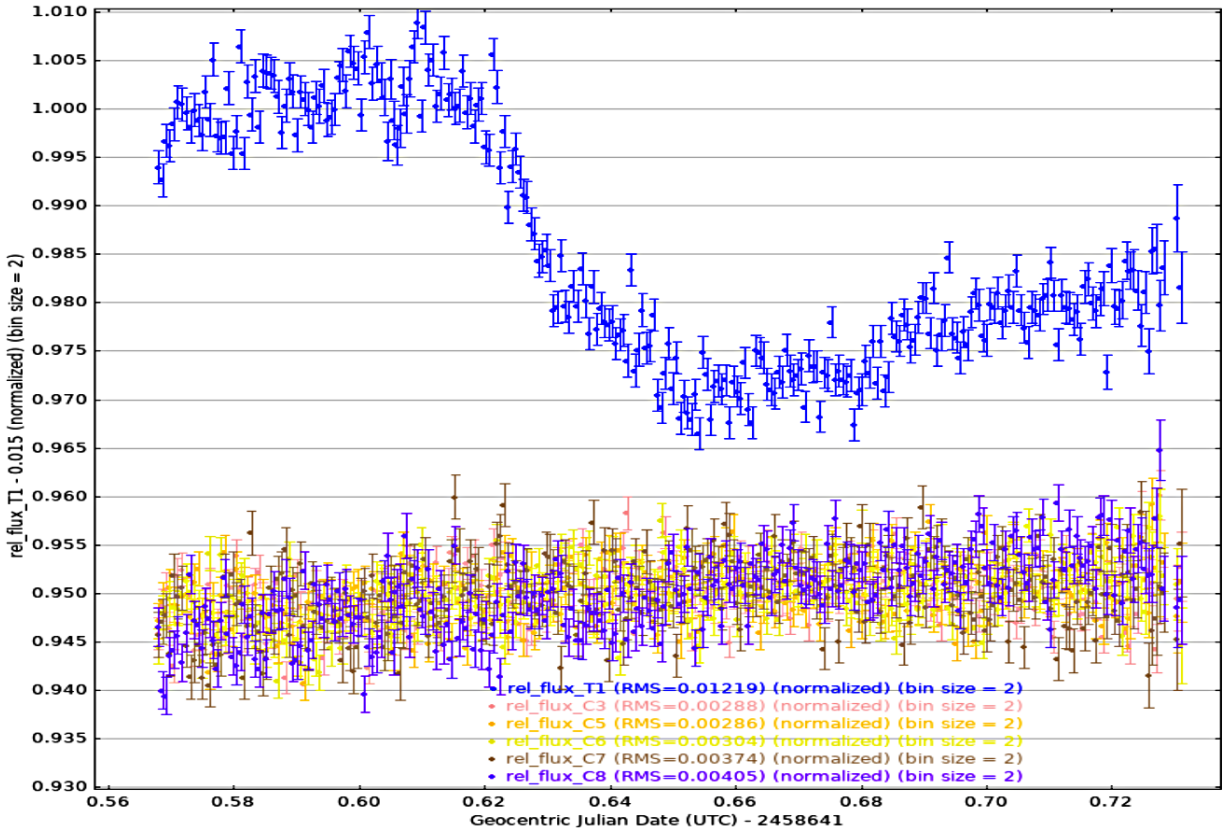

Figure 10a. Comparison of the light curve from Gaia DR2 1864883699097368448 and the first 6 of the 21 comparison stars used to obtain these light curves. Binning is set to 2 on AIJ for this plot. As can be seen there is a clear linear trend to all of the stars in this image, which was removed to measure the depth seen in the target star's light curve.

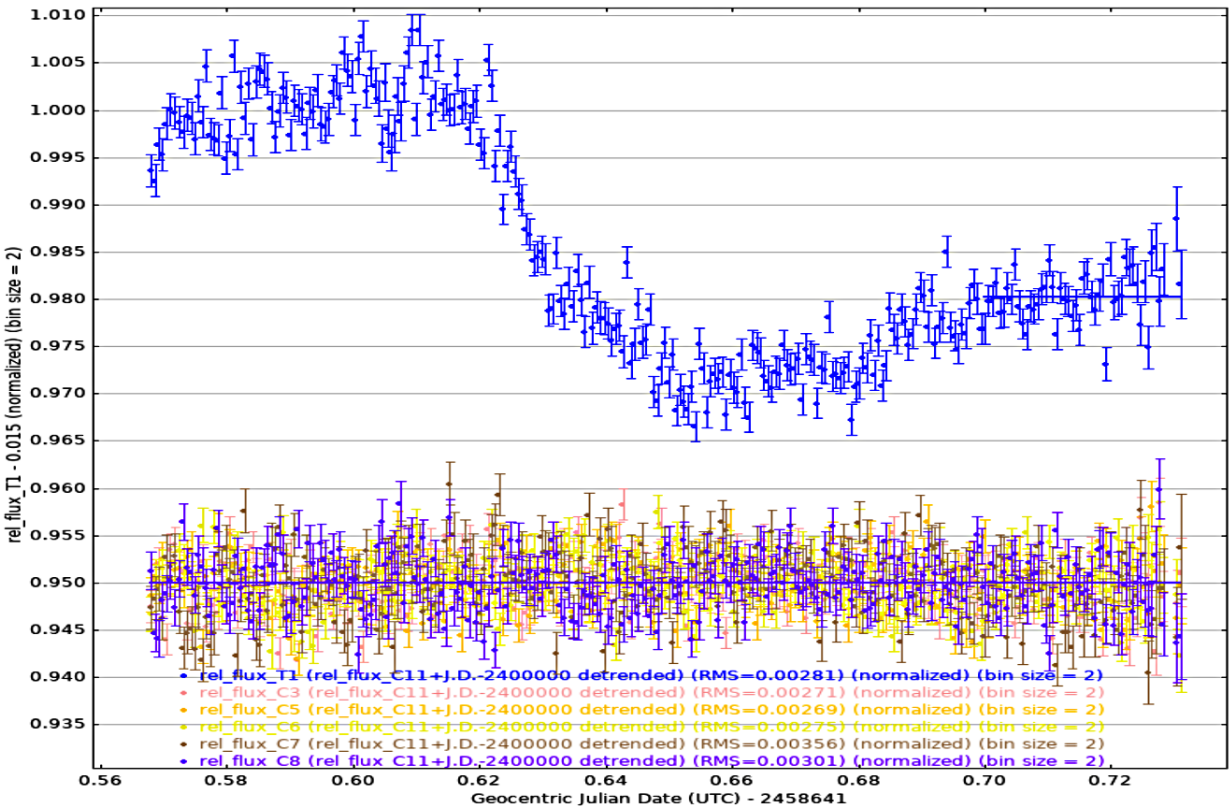

Figure 10b. Detrended Gaia DR2 1864883699097368448 and comparison star light curves, detrended using AIJ.

Table 5. Variable candidate periods and magnitude estimates.

Designation	*Star*	*R-Band Apparent Mag.*	*ASAS-SN/ZTF Survey Period (days)*	*Reanalysis of ASAS-SN V-band Period (days)*	*Our R-band Period (days)*	*Classification*
V1	ASASSN-V J205658.12 +314215.9	14.8 ± 0.02	0.7543	0.7544 ± 0.0002	0.7643 ± 0.0009	EW
V2	ASASSN-V J205552.88 +314615.9	14.1 ± 0.02	0.6002	0.8586 ± 0.0071	0.4388 ± 0.0005	EW
V3	2MASS J20564622+3138394	14.0 ± 0.02	—	—	0.3465 ± 0.0005	EW
V4	2MASS J20560314+3145505	17.1 ± 0.02	—	—	0.3021 ± 0.0006	EW
V5	ZTF J205733.78+314612.6	16.4 ± 0.02	0.4251	—	0.4282 ± 0.0007	EW
V6	ZTF J205627.42+315322.4	16.9 ± 0.02	0.2925	—	0.2981 ± 0.0004	EW
V7	2MASS J20562743+3153225	17.7 ± 0.04	—	—	0.2963 ± 0.0005	Possible EW

Note: As mentioned before, error estimates were not provided for the ASAS-SN and the ZTF survey periods. (Jayasinghe et al. *2018, 2019; Masci* et al. *2019; Chen* et al. *2020).*

Table 6. Gaia information on the possible transit star.[1]

Gaia Designation	*R.A.* °	*Dec.* °	*Parallax (mas)*	*Distance (pc)*	*Temperature K*	*Radius ($R_\odot$)*	*Luminosity ($L_\odot$)*
DR2 1864883699097368448	314.190	31.617	0.965 ± 0.018	$1036.4^{+19.3}_{-18.6}$	6224^{+63}_{-233}	$1.480^{+0.117}_{-0.030}$	2.962 ± 0.153

[1] *From Gaia Collaboration* et al. *(2016, 2018), NASA/IPAC (2020).*

As with the other variable star candidates discussed in the previous sections, we examined the region on the charge-coupled device (CCD) near the star's position, and were able to rule out bad columns or other CCD artifacts affecting the light curve.

The shape of the light curve seen in Figures 10a and 10b, suggests an eclipsing binary system or exoplanet transit. If this is indeed the case, these observations span the ingress phase and an addition 100 minutes until terminated by the approaching dawn. No egress was seen.

As can be seen in Figures 10a and 10b there appears to be a linear trend to not only the target star but the comparison stars as well. After correcting for this trend, the overall depth of the minima is 4.1% of the total flux of the star.

Based on the stellar radius estimate from the Gaia database, listed in Table 6, this star is larger than the sun. If we assume this variation is indeed caused by a transit, we can estimate the planet's radius to be:

$$R_p = 2.98^{+0.35}_{-0.09} R_{Jupiter}$$

Because of the overall depth of the variation, it appears to be more likely to be an eclipsing binary system than an exoplanet transit, although such size is not without precedent for planets, as the directly imaged exoplanet GQ Lupi b was estimated to be 3 Jupiter radii (Neuhäuser *et al.* 2008).

4. Conclusions

In this paper we presented evidence for three new variable stars in the field around the star KELT-16. We provided period estimates for each of these three newly detected variable stars. Based on these periods and their light curves we classified them as likely contact binary stars. Each of the periods for these three stars were less than a day, with the periods ranging from 0.3 to 0.5 day. Additionally, we provided photometry and period analysis of four previously known variable stars in this field.

Finally, on one night, another field star showed a dimming similar to an eclipsing binary system or an exoplanet transit. Either additional observations of this star or a search through archival observations of this region will be necessary to confirm both the existence of this object and whether it is planetary or stellar in nature.

5. Acknowledgements

We thank Ball State University and the SARA consortium for providing the observatories and the observing time used in this search without which this research would not have been possible.

Additionally, this work made use of public data provided by both the ASAS-SN survey and the ZTF survey during our V-band analysis and as a check for our R-band analysis, respectively.

Finally, thank you to the anonymous referee for their valuable comments during the referee process.

References

Chen, X., Deng, L., de Grijs, R., Wang, S., and Feng, Y. 2018, *Astrophys. J.*, **859**, 140.

Chen, X., Wang, S., Deng, L., de Grijs, R., Yang, M., and Tian, H. 2020, *Astrophys. J., Suppl. Ser.*, **249**, 18.

Collins, K. A., Kielkopf, J. F., Stassun, K. G., and Hessman, F. V. 2017, *Astron. J.*, **153**, 77 (arXiv:1701.04817v1).

Gaia Collaboration, *et al.* 2016, *Astron. Astrophys.*, **595A**, 1.

Gaia Collaboration, *et al.* 2018, *Astron. Astrophys.*, **616A**, 1.

Harris, A. W., *et al.* 1989, *Icarus*, **77**, 171.

Henden, A. A., and Kaitchuck, R. H. 1990, *Astronomical Photometry: A Text and Handbook for the Advanced Amateur and Professional Astronomer*, Willmann-Bell, Richmond, VA.

Jayasinghe, T., *et al.* 2018, *Mon. Not. Roy. Astron. Soc.*, **477**, 3145.

Jayasinghe, T., *et al.* 2019, The ASAS-SN Catalog of Variable Stars VI (arXiv:1910.14187v1), (https://asas-sn.osu.edu/variables/AP10960259), (https://asas-sn.osu.edu/variables/AP10971522).

Keel, W. C., *et al.* 2016, "The Remote Observatories of the Southeastern Association for Research in Astronomy (SARA)", (arXiv:1608.06245).

Kunimoto, M., and Matthews, J. M. 2020, *Astron. J.*, **159**, 248.

Masci, F. J., *et al.* 2019, *Publ. Astron. Soc. Pacific*, **131**, 018003.

NASA/IPAC Infrared Science Archive (IRSA). 2020 (https://irsa.ipac.caltech.edu).

Neuhäuser, R., Mugrauer, M., Seifahrt, A., Schmidt, T. O. B., and Vogt, N. 2008, *Astron. Astrophys.*, **484**, 281.

Oberst, T. E., *et. al.* 2017, *Astron. J.*, **153**, 97.

Paunzen, E., and Vanmunster, T. 2016, *Astron. Nachr.*, **337**, 239 (arXiv:1602.05329).

Rucinski, S. M. 1994, *Publ. Astron. Soc. Pacific*, **106**, 462.

Schwarzenberg-Czerny, A. 1996, *Astrophys. J., Lett.*, **460**, L107.

Shappee, B. J., *et al.* 2014, *Astrophys. J.*, **788**, 48.

Sokolovsky, K. V., and Lebedev A. A. 2017, VaST: Variability Search Toolkit, Astrophysics Source Code Library, record ascl:1704.005.

Sravan, N., Marchant, P., and Kalogera, V. 2019, "Progenitors of Type IIb Supernovae: I. Evolutionary Pathways and Rates" (arXiv:1808.07580v2).

Stellingwerf, R. F. 1978, *Astrophys. J.*, **224**, 953.

Valdes, F. 1988, in *Instrumentation for Ground-Based Optical Astronomy: Present and Future—The 9th Santa Cruz Summer Workshop in Astronomy and Astrophysics, July 13–July 24, 1987, Lick Observatory,* ed. L. B. Robinson, Springer-Verlag, New York, 417.

Vanmunster, T. 2006, light curve and period analysis software, peranso v.2.0 (http://www.cbabelgium.com/peranso).

Zacharias, N., *et al.* 2010, *Astron. J.*, **139**, 2184.